# Thermophilic *Talaromyces emersonii* Flavin Adenine Dinucleotide-Dependent Glucose Dehydrogenase Bioanode for Biosensor and Biofuel Cell Applications

Hisanori Iwasa,[†] Atsunori Hiratsuka,[†] Kenji Yokoyama,[†,‡] Hirotaka Uzawa,[†] Kouhei Orihara,[§] and Hitoshi Muguruma*[,§]
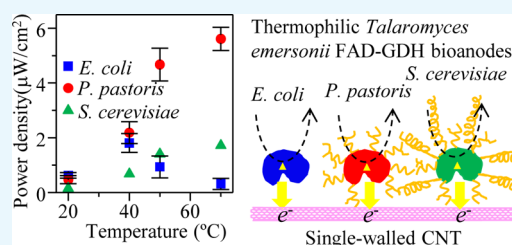
[†]Nanomaterials Research Institute, National Institute of Advanced Industrial Science and Technology (AIST), Central 5-41, 1-1-1 Higashi, Tsukuba, Ibaraki 305-8565, Japan

[‡]School of Bioscience and Biotechnology, Tokyo University of Technology, 1404-1 Katakura, Hachioji, Tokyo 192-0982, Japan

[§]Graduate School of Engineering and Science, Shibaura Institute of Technology, 3-7-5 Toyosu, Koto, Tokyo 135-8548, Japan

**S** *Supporting Information*

**ABSTRACT:** Flavin adenine dinucleotide (FAD)-dependent glucose dehydrogenase (GDH) was identified and cloned from thermophilic filamentous fungi *Talaromyces emersonii* using the homology cloning method. A direct electron transfer bioanode composed of *T. emersonii* FAD-GDH and a single-walled carbon nanotube was produced. Enzymes from thermophilic microorganisms generally have low activity at ambient temperature; however, the *T. emersonii* FAD-GDH bioanode exhibits a large anodic current due to the enzymatic reaction (1 mA cm$^{-2}$) at ambient temperature. Furthermore, the *T. emersonii* FAD-GDH bioanode worked at 70 °C for 12 h. This is the first report of a bioanode with a glucose-catalyzing enzyme from a thermophilic microorganism that has potential for biosensor and biofuel cell applications. In addition, we demonstrate how the glycoforms of *T. emersonii* FAD-GDHs expressed by various hosts influence the electrochemical properties of the bioanode.

## INTRODUCTION

Thermostable enzymes from thermophilic microorganisms display not only heat and chemical resistance but also excellent long-term storage tolerance. The application of thermostable enzymes is promising and has been reported by some researchers.[1−6] However, the application of a thermostable enzyme to catalyze glucose, which is one of the most important substrates in the fields of medicine, biochemistry, environmental science, fermentation, and agriculture, has not yet been reported. *Talaromyces emersonii* is a thermophilic filamentous fungus and is a natural saprophyte that inhabits soil and compost heaps. Highly specific thermostable enzyme cocktails produced by *T. emersonii* have been applied to the baking of bread.[7] However, *T. emersonii* does not secrete a glucose-catalyzing enzyme under conventional cultivation conditions. We have identified and cloned flavin adenine dinucleotide (FAD)-dependent glucose dehydrogenase (GDH) from *T. emersonii* using the homology cloning method.[8]

Oxygen-insensitive FAD-GDH has attracted considerable attention over the past several years, and there are increasing reports of biosensors and biofuel cells that employ FAD-GDH.[9−24] FAD-GDH used in such biodevices is typically isolated from *Aspergillus*,[9−20] *Glomerella*,[21,22] or *Burkholderia*;[23,24] however, FAD-GDHs from these sources exhibit inadequate thermal stability and substrate selectivity, and they give rise to several practical problems. Consequently, an FAD-GDH suitable for biodevice applications such as biosensors and biofuel cells has not yet been identified. In this article, we present the characterization of a thermophilic *T. emersonii* FAD-GDH bioanode for biosensor and biofuel cell applications.

## RESULTS AND DISCUSSION

**Characterization of *T. emersonii* FAD-GDHs Expressed by Various Hosts.** Recombinant *T. emersonii* FAD-GDHs were expressed in the bacterium *Escherichia coli* (*Ec*GDH) and the yeasts *Pichia pastoris* (*Pp*GDH) and *Saccharomyces cerevisiae* (*Sc*GDH) because the collection of FAD-GDHs from the original host is thought to be difficult. The recombinant proteins expressed in the yeasts have different glycoforms; thus, the FAD-GDHs have different molecular masses (*Ec*GDH: 60 kDa; *Pp*GDH: 90−150 kDa; *Sc*GDH: 110−250 kDa). The FAD-GDHs used in this research are summarized in Table S1 in the Supporting Information, and the results of sodium dodecyl sulfate polyacrylamide gel electrophoresis (SDS-PAGE) separation are shown in Figure 1. Recombinant proteins expressed by the three hosts differ in their glycan chain amount, and their glycan chain lengths increase in the order *Sc*GDH > *Pp*GDH > *Ec*GDH. Expression in prokaryotic *E. coli*, which cannot glycosylate proteins, is equivalent to removal of the glycosyl groups. The molecular mass of GDH
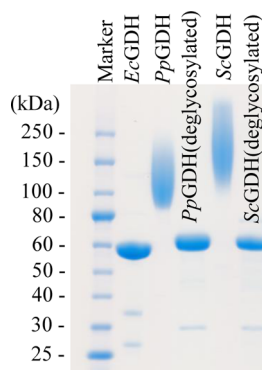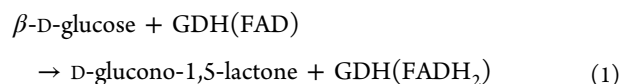
**Figure 1.** SDS-PAGE results for *T. emersonii* FAD-GDHs used herein.

without glycan chains is 60 kDa, which is the same as the molecular mass of *Ec*GDH. The apparent mass of the glycan chains in *Pp*GDH and *Sc*GDH is between 50−183% and 83−317% that of the peptide chain, respectively. Glycan chains are mainly composed of high mannose-type oligosaccharides that contain mannose and *N*-acetylglucosamine.[25,26] These oligosaccharide chains connect to asparagine, threonine, and serine residues on the surface of GDH. The difference in the amount of glycan chains in *Pp*GDH and *Sc*GDH is attributed to *S. cerevisiae*-expressed proteins often being hyperglycosylated, where each oligosaccharide can contain more than 50 mannose residues.[25] The judicious choice of hosts is thus an unavoidable step in the utilization of enzymes by homology cloning.

**Characterization of Bioanode with *T. emersonii* FAD-GDHs.** The electrochemical performance of a bioanode is largely governed by the efficiency of electron transfer between the enzyme and the electrode (electron collector). The crystal structure of FAD-GDH from *Aspergillus flavus* has recently been solved.[27] The FAD cofactor in GDH is tightly and deeply embedded within a structurally rigid glycoprotein shell. Adopting the configuration for electron transfer is thought to be an unavoidable task in FAD-GDH. There are two approaches for electron transfer to occur. One is to utilize electron transfer mediators, which are often small and mobile agents such as hexacyanoferrate(III),[13] octacyanomalybdate,[12] osmium complexes,[10,21,22] phenothiazine,[11,15] or menadione.[14] The problem with mediated electron transfer (MET) is that the mediators can leach out, reducing the sensitivity of this process and causing poisoning problems. Even if immobilized and polymeric mediators are adopted, the complicated process, which includes the preparation of an accommodating polymer matrix and the need to fine tune the hydrophobic mediator and

hydrophilic enzyme, is not avoidable. The other approach is direct electron transfer (DET). We have previously reported that DET occurs between a single-walled carbon nanotube (SWNT) and FAD-GDH from *A. oryzae*, the amino acid sequence of which perfectly corresponds to that of *A. flavus* FAD-GDH.[9] Therefore, DET is expected to take place with the fabricated *T. emersonii* FAD-GDH bioanodes. To clearly evaluate the utility of these FAD-GDHs, a simple layer-by-layer process based on a SWNT and a plasma-polymerized thin film (PPF)[28,29] was adopted, as shown in Figure 2. The DET electrode has a sandwich-like structure of PPF/GDH/SWNT/PPF/Au. The first PPF layer on the Au electrode acts as a scaffold for the formation of the SWNT layer. A SWNT layer cannot be obtained without the PPF layer being there first. The anionic surfactant sodium cholate disrupts the SWNT bundles into individual SWNT molecules. Figure 2A shows an atomic force microscopy (AFM) image of the surface of the SWNT layer (SWNT/PPF/Au) and shows that the SWNT network is formed by unbundled SWNT molecules.[29] Figure 2B shows an AFM image of the GDH immobilized surface (PPF/GDH/SWNT/PPF/Au). As can be seen, GDH percolates into the SWNT and forms a SWNT−GDH complex, probably because the protein itself aids in stabilizing a SWNT dispersion.

Cyclic voltammograms (CVs) of bioanodes prepared with *T. emersonii* FAD-GDH expressed in three hosts (*Ec*GDH, *Pp*GDH, and *Sc*GDH) at 20 °C are shown in Figure 3A. Glucose concentration vs current plots using the CV data are shown in Figure S1. The glucose-concentration-dependent current (GCDC) output due to the increase in the polarized potential increases steeply, and the oxidative current starts at around +0.1 V (onset potential). DET between FAD-GDH and a SWNT is represented by

$$\beta\text{-D-glucose} + \text{GDH(FAD)}$$
$$\rightarrow \text{D-glucono-1,5-lactone} + \text{GDH(FADH}_2) \qquad (1)$$

$$\text{GDH(FADH}_2) \rightarrow \text{GDH(FAD)} + 2\text{H}^+ + 2\text{e}^- \qquad (2)$$

FAD-GDH has only one enzyme-catalytic pathway (eqs 1 and 2). The GCDC at +0.4−0.8 V is not due to hydrogen peroxide because oxygen-insensitive FAD-GDH does not produce hydrogen peroxide. Therefore, the observation of a large GCDC at +0.4−0.8 V is evidence of DET between FAD-GDH and the SWNT. A quantum tunneling current due to an overpotential is the reason that GCDC did not appear at −0.45 V (redox potential of FAD) but did appear at +0.4−0.8 V.[9]
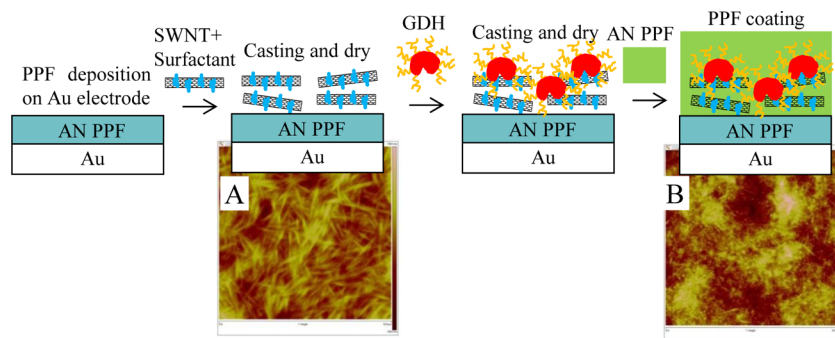


**Figure 2.** Illustration of the SWNT−GDH electrode preparation process. AFM images of a (A) SWNT layer on PPF/Au and (B) GDH-immobilized surface on a SWNT layer. Horizontal scale: (A, B) $10 \times 10$ mm$^2$. Vertical scale: (A) 300 nm and (B) 20 nm.
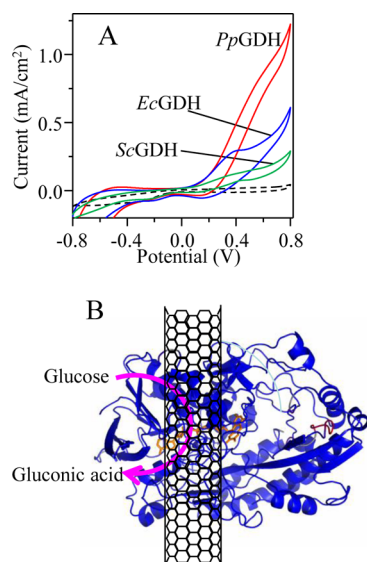
**Figure 3.** (A) CV profiles for the *T. emersonii* FAD-GDH anodes at 20 °C. The glucose concentration was 48 mM. The dashed line represents the background current. Sweep rate: 50 mV s$^{-1}$. The electrolyte was pH 7.4 phosphate buffer solution. (B) Speculative DET model between FAD-GDH and SWNT. The diameter of the SWNT is 1.2 nm. The three-dimensional structure of *T. emersonii* FAD-GDH was modeled based on the structure of *A. flavus* FAD-GDH[27] using the SWISS-MODEL server.[30]

The entire sequence of *T. emersonii* FAD-GDH is different from that of *A. flavus* FAD-GDH (64.2% sequence identity). However, both the structure and size of *T. emersonii* FAD-GDH were almost the same as those of *A. flavus* FAD-GDH, with a global model quality estimation score of 0.76, which suggests that the modeled structure is highly reliable. Three-dimensional structure modeling of *T. emersonii* FAD-GDH was performed based on the structure of *A. flavus* FAD-GDH[27] using the SWISS-MODEL server.[30] The overall FAD-GDH molecule is a 4.5 × 5.6 × 7.8 nm$^3$ globular structure. FAD is positioned 1.4 nm from the surface. A feasible scheme for this involves the side wall of the SWNT being plugged into the groove of FAD-GDH, as shown in Figure 3B, where the SWNT axis is embedded in the surface of the electrode and FAD-GDH has a groove into which a 1.2 nm diameter individual SWNT can enter. The individual SWNT can thus be close to a distance of 1.0 nm from the FAD positioned at the bottom of the groove in Figure 3B. We think that there is no possibility that the SWNT "docking" to FAD-GDH will block the substrate's access. There is space for the substrate (glucose) to gain access because a large GCDC is observed. Also, there is no possibility that the glycan shell will act like a spacer because the GCDC of the bioanode with a glycan-chain-rich enzyme is much larger than that using an enzyme with no glycan chain. Therefore, it is feasible that the current at +0.4−0.8 V is a tunneling current from FAD.

The markedly larger response of the *Pp*GDH glycoprotein anode than that of the *Ec*GDH deglycosylated protein is contrary to our expectation because (i) the activity of *Ec*GDH is larger than that of *Pp*GDH (Table S1) and (ii) the common strategy for MET is deglycosylation in order to shorten the distance between the electrode and the FAD cofactor in GDH.[10,11,22] This suggests that the strategy for controlling the glycan chain is different between DET and MET. It is possible that one role of the glycan chains is to stabilize the tertiary

structure of the protein. The *Ec*GDH deglycoprotein is less robust than the *Pp*GDH glycoprotein; thus, *Ec*GDH in close proximity to a SWNT may unfold and lose its activity. Conversely, the response of the *Sc*GDH anode is markedly smaller than that of the *Pp*GDH anode, possibly due to there being fewer enzymes undergoing DET on the *Sc*GDH anode than on the *Pp*GDH electrode because the thicker glycan shell on *Sc*GDH prevents the SWNT from being in close proximity to the FAD cofactor.

**Biofuel Cell.** Next, the performance of the *T. emersonii* FAD-GDH bioanode was tested in a biofuel cell. A platinum electrode was used as the cathode to eliminate limitations from the cathode. Figure 4A shows the polarization curve and power
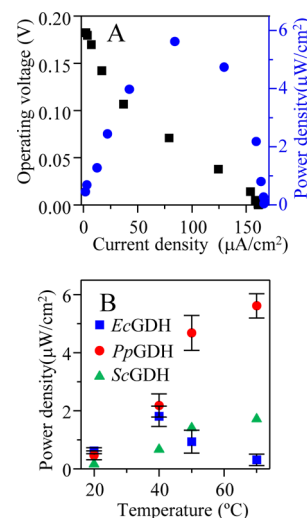


**Figure 4.** (A) Polarization curve (black dots) and output power (blue dots) of a biofuel cell with the *T. emersonii* FAD-GDH (*Pp*GDH) anode at 70 °C. Platinum wire was used as the cathode. (B) Maximum output power of bioanodes with *T. emersonii* FAD-GDH expressed by various hosts as a function of temperature. The glucose concentration was 19 mM. The electrolyte was pH 7.4 phosphate buffer solution.

output of a biofuel cell constructed from a *Pp*GDH anode. The *Pp*GDH anode can function at a high temperature (70 °C). Furthermore, it works continuously for 12 h, as shown in Figure S2. Tsujimura et al.[10] demonstrated that support by a hydrogel/mesoporous carbon matrix stabilizes the FAD-GDH structure, allowing functionality at temperatures up to 55 °C to be achieved with a typical FAD-GDH bioanode. There is no effect of having a matrix support with the layer-by-layer immobilization procedure used in the present work. Therefore, this is typical of a thermostable enzyme from a thermophilic microorganism. If this system is combined with a biocathode that has a thermostable enzyme,[1] then a biofuel cell with long-term stability and high temperature resistance would be realized.

Figure 4B shows the maximum output power of *T. emersonii* FAD-GDHs from various hosts as a function of temperature. The output power of the *Pp*GDH bioanode is larger than that of the *Ec*GDH bioanode at all temperatures, which corresponds to the CV data in Figure 3A. For the *Pp*GDH bioanode, a higher temperature results in a higher output power. The output power vs temperature plot of the *Pp*GDH anode is similar to the enzymatic activity vs temperature plot for free *Pp*GDH.[8] In contrast, the output power of the *Ec*GDH bioanode decreased when the temperature surpassed 40 °C.

The output power vs temperature plot for the *Ec*GDH anode is different from the enzymatic activity vs temperature plot for free *Ec*GDH, where the activity increased up to 60 °C. The fragility of the tertiary structure in the *Ec*GDH/SWNT complex is consistent with the CV data for the *Ec*GDH/SWNT bioanode in Figure 3A.

For the *Sc*GDH bioanode, although the output is smaller than that for the *Pp*GDH anode, it increased with the temperature, which suggests that the glycan chains prevent the enzyme from unfolding and embedding in the SWNT under harsh conditions such as heating. *Pp*GDH contains a suitable number of glycan chains, which allows DET to occur without unfolding. However, the thermostability of *Pp*GDH is attributed not only to the presence of glycan chains but also to its sequence. This is supported by the decrease in the output power of the bioanode using normal FAD-GDH that has glycan chains when the temperature surpassed 40 °C. Thus, the output power vs temperature profile for the glycosylated FAD-GDH anode from a nonthermophilic microorganism was similar to that for the *Ec*GDH anode. It is thus concluded that *Pp*GDH contains a suitable number of glycan chains, which allows the SWNT to closely approach FAD without *Pp*GDH unfolding.

**Biosensor.** The performance of the *Pp*GDH anode as a biosensor was evaluated. Amperometric measurements at a fixed potential are widely used to evaluate and analyze the performance of *Pp*GDH anodes as a glucose biosensor. Figure 5A shows the steady-state amperometric response of the
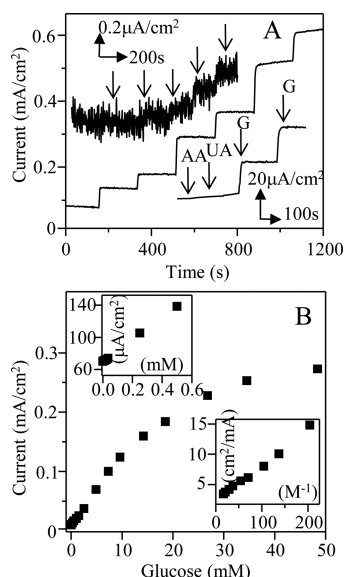


**Figure 5.** (A) Time−current response of the *Pp*GDH anode with the sequential addition of glucose at concentrations of 0.25, 0.5, 1.0, 1.5, 2.5, and 3.5 mM. The temperature was set at 20 °C. Upper inset: Time−current response for sequential glucose additions at concentrations of 5, 10, 15, 25, and 35 mM. Bottom inset: Effect of an interfering species [0.1 mM ascorbic acid (AA); 0.1 mM uric acid (UA)] on the response of the *Pp*GDH anode. The concentrations of glucose (G) were 1 and 2 mM, sequentially. The polarization potential was +0.6 V vs Ag/AgCl with a pH 7.4 electrolyte of 20 mM phosphate buffer solution. (B) Calibration plot for glucose response using the data in panel A. The sensitivity of the electrode was 10 $\mu$A mM$^{-1}$ cm$^{-2}$ ($r$ = 0.99 in the linear range of 0.005−27 mM). Upper inset: Calibration plot for a very low concentration range. Lower inset: Lineweaver−Burk plot ($I_{max}$ = 0.43 mA cm$^{-2}$, $K_M^{app}$ = 22 mM) generated using eq 3.

*Pp*GDH anode at +0.6 V vs Ag/AgCl at 20 °C. The current at +0.6 V is available for time-based measurement with a fixed potential. A sequential increase in the electrochemical signal with the increase of the glucose concentration at regular intervals is observed, and the glucose concentration range evaluated covers the physiological range. The response time was 6 s. The detection characteristics at very low concentrations (5−35 $\mu$M) are good, and the detection limit (signal/noise ratio = 2) was 5 $\mu$M (upper inset of Figure 5A). The effects of interfering compounds such as ascorbic acid and uric acid on the sensing characteristics are negligible (bottom inset of Figure 5A), which suggests that the *Pp*GDH electrode can be used with physiological samples.

Figure 5B shows a plot of current vs glucose concentration based on the data from Figure 5A. Table S2 shows the characteristics and performance of the biosensors with FAD-GDH from a thermophilic microorganism compared with those for other FAD-GDHs from nonthermophilic counterparts. The sensitivity determined from the slope for the *Pp*GDH bioanode was 10 $\mu$A mM$^{-1}$ cm$^{-2}$ ($r$ = 0.98 in the linear range of 0.005−26 mM). It is significant that the biosensor with a thermophilic *T. emersonii* FAD-GDH bioanode can work at ambient temperature, similar to a normal FAD-GDH bioanode. It is also noteworthy that a wider dynamic range, from the detection limit to a glucose concentration indicative of diabetes, was observed compared to that of other FAD-GDH biosensors, which is a unique characteristic of biosensors with a thermophilic *T. emersonii* FAD-GDH anode (upper inset of Figure 5B). Deviation from linearity is observed at high (>30 mM) glucose concentrations, a typical characteristic of the Michaelis−Menten model. This is a reaction-controlled step and can thus be analyzed using the Michaelis−Menten model. The bottom inset of Figure 5B shows a Lineweaver−Burk plot, from which the apparent Michaelis−Menten activity ($K_m^{app}$) can be calculated to provide an indication of the enzyme−substrate kinetics of the biosensor

$$\frac{1}{I} = \frac{K_m^{app}}{I_{max}}\frac{1}{C} + \frac{1}{I_{max}} \tag{3}$$

where $I$ is the steady-state current, $I_{max}$ is the maximum current under stationary substrate conditions, $K_m^{app}$ denotes the apparent Michaelis constant, and $C$ is the glucose concentration. $I_{max}$ and $K_m^{app}$ were obtained by extrapolation of the plot. The large $I_{max}$ (0.43 mA cm$^{-2}$) is indicative of a highly effective electronic contact. $K_m^{app}$ for immobilized *Pp*GDH was estimated to be 22 mM, which is significantly smaller than that for *Pp*GDH in solution ($K_m$ = 337 mM). The operational stability and storage stability were confirmed. A current response greater than 90% was retained for 12 h. The response was retained over the period of 7 days by storing at room temperature. The results demonstrate several advantages of this electrode: (i) *Pp*GDH is suitable for use in biosensor applications, despite its low affinity toward the substrate, i.e., large $K_m$; (ii) this low affinity toward the substrate means that a wide sensing dynamic range is obtained without the need to control diffusion, such as with a membrane; and (iii) despite being an enzyme from a thermophilic microorganism, *Pp*GDH can be used at ambient temperature.

## ■ CONCLUSIONS

We have reported a bioanode with thermophilic filamentous fungi *T. emersonii* FAD-GDH for biosensor and biofuel cell

applications. *T. emersonii* FAD-GDH was expressed in the bacterium *E. coli* and yeasts *P. pastoris* and *S. cerevisiae* and was obtained in different glycoforms. Although enzymes from thermophilic microorganisms typically have low activity at lower temperature, GCDC at an electrode incorporating a *T. emersonii* FAD-GDH anode was observed. The *T. emersonii* FAD-GDH (*Pp*GDH) bioanode also functioned at 70 °C for 12 h. It is possible that having a suitable amount of glycan chains at the FAD-GDH interface prevents electron transfer between FAD and the SWNT from being disturbed while also preventing denaturation of the enzyme at high temperature. This is the first report that a bioanode with a glucose-catalyzing enzyme from a thermophilic microorganism can be applied to biosensors and biofuel cells.

## ■ EXPERIMENTAL SECTION

**Materials and Reagents.** Distilled water, potassium dihydrogen phosphate, disodium hydrogen phosphate, D-glucose, L-ascorbic acid, uric acid, acetonitrile, and anionic surfactant sodium cholate (SC) were purchased from Kanto Chemical Co., Inc. (Tokyo, Japan). Single-walled carbon nanotubes (SWNT; 1.2−1.7 nm in diameter, 0.5 mm average length, Super Pure Tubes) were purchased from Nanointegris Inc. (Boisbrin, Canada). FAD-GDH (EC 1.1.5.9) from thermophilic *T. emersonii* was identified by our group.[8] Recombinant *T. emersonii* FAD-GDHs were expressed by the bacterium *E. coli* and yeasts *P. pastoris*[8] and *S. cerevisiae*. The *S. cerevisiae* INVSc1 strain and pYES2 expression vector were purchased from Thermo Fisher Scientific (Waltham, USA). In both yeast expression systems, the $\alpha$-factor secretion signal was fused to FAD-GDH, and FAD-GDH was secreted into the culture media. FAD-GDH was purified by methods from our group.[8]

**Electrode Preparation.** The electrochemical device as a working electrode was fabricated using a layer-by-layer process. The device was formed on sputtered Au. The width of the opening for the working electrode was 9 mm². An ULVAC VEP-1000 plasma generator was used to deposit a 2 nm thick acetonitrile PPF layer onto Au. A SWNT/sodium cholate solution (1.5 mg mL$^{-1}$ and 20 mg mL$^{-1}$, respectively) was dropped onto the PPF surface and dried in a vacuum oven. The thickness of the resulting sorted SWNT film was ca. 120 nm. Subsequently, the SWNT adsorbed surface was treated by acetonitrile plasma using the following parameters: power, 100 W; flow rate, 15 mL min$^{-1}$; pressure, 0.6 Pa; and exposure time, 30 s (thickness < 1 nm). The role of PPF is surface modification and then layer formation (polymerization). The enzyme solution (3−10 mL) was then added by dropping an aliquot of enzyme in phosphate buffer (20 mM, pH 7.4) onto the film. All enzyme solutions for drop-casting contain 100 units. One hour later, the device was washed with water. Finally, the enzyme-adsorbed surface was overcoated with a 6 nm thick acetonitrile PPF layer (second layer). The deposition parameters were as follows: power; 150 W, pressure; 0.6 Pa, and exposure time; 150 s. The devices were stored in a refrigerator at 4 °C until use.

**Measurements.** AFM was conducted in tapping mode in an air atmosphere using a NanoScope V Dimension Icon stage system produced by Bruker AXS GmbH (Karlsruhe, Germany). The scanning rate was 0.33−1.0 Hz. Electrochemical measurements were performed with an electrochemical analyzer (ALS Instruments, 701A, West Lafayette, IN) using a three-electrode configuration. Reference (Ag/AgCl, RE-1C) and counter (platinum wire, cathode) electrodes were purchased from Bioanalytical Systems Inc. Electrochemical measurements were conducted in a 5 mL vessel at ambient temperature (20 °C) using phosphate buffer (20 mM, pH 7.4) as the supporting electrolyte. To prepare samples at designated concentrations, stock glucose solutions of 2.5, 25, or 250 mM were successively added.

## ■ ASSOCIATED CONTENT

## ■ AUTHOR INFORMATION

**Corresponding Author**
*E-mail: muguruma@shibaura-it.ac.jp.

**ORCID** 
Hitoshi Muguruma: 0000-0001-5213-2062

**Notes**
The authors declare no competing financial interest.

## ■ REFERENCES

(1) Holmberg, S.; Rodriguez-Delgado, M.; Milton, R. D.; Ornelas-Soto, N.; Minteer, S. D.; Parra, R.; Madou, M. J. Bioelectrochemical Study of Thermostable *Pycnoporus sanguineus* CS43 Laccase Bioelectrodes Based on Pyrolytic Carbon Nanofibers for Bioelectrocatalytic O₂ Reduction. *ACS Catal.* **2015**, *5*, 7507−7518.

(2) de Poulpiquet, A.; Ciaccafava, A.; Gadiou, R.; Gounel, S.; Giudici-Orticoni, M. T.; Mano, N.; Lojou, E. Design of A H₂/O₂ Biofuel Cell Based on Thermostable Enzymes. *Electrochem. Commun.* **2014**, *42*, 72−74.

(3) Shi, L.; Liu, X.; Niu, W.; Li, H.; Han, S.; Chen, J.; Xu, G. Hydrogen Peroxide Biosensor Based on Direct Electrochemistry of Soybean Peroxidase Immobilized on Single-Walled Carbon Nanohorn Modified Electrode. *Biosens. Bioelectron.* **2009**, *24*, 1159−1163.

(4) Özkan, M.; Erhan, E.; Terzi, Ö.; Tan, İ.; Özöner, Ş. K. Thermostable Amperometric Lactate Biosensor with *Clostridium thermocellum* L-LDH for The Measurement of Blood Lactate. *Talanta* **2009**, *79*, 1412−1417.

(5) Iyer, R.; Pavlov, V.; Katakis, I.; Bachas, L. G. Amperometric Sensing at High Temperature with A"Wired" Thermostable Glucose-6-phosphate Dehydrogenase from *Aquifex aeolicus*. *Anal. Chem.* **2003**, *75*, 3898−3901.

(6) Jeffries, C.; Pasco, N.; Baronian, K.; Gorton, L. Evaluation of A Thermophile Enzyme for A Carbon Paste Amperometric Biosensor: L-Glutamate Dehydrogenase. *Biosens. Bioelectron.* **1997**, *12*, 225−232.

(7) Waters, D. M.; Murray, P. G.; Ryan, L. A.; Arendt, E. K.; Tuohy, M. G. *Talaromyces emersonii* Thermostable Enzyme Systems and Their Applications in Wheat Baking Systems. *J. Agric. Food Chem.* **2010**, *58*, 7415−7422.

(8) Ozawa, K.; Iwasa, H.; Sasaki, N.; Kinoshita, N.; Hiratsuka, A.; Yokoyama, K. Identification and Characterization of Thermostable Glucose Dehydrogenase from Thermophilic Filamentous Fungi. *Appl. Microbiol. Biotechnol.* **2017**, *101*, 173−183.

(9) Muguruma, H.; Iwasa, H.; Hidaka, H.; Hiratsuka, A.; Uzawa, H. Mediatorless Direct Electron Transfer between Flavin Adenine Dinucleotide-Dependent Glucose Dehydrogenase and Single-Walled Carbon Nanotubes. *ACS Catal.* **2017**, *7*, 725−734.

(10) Tsujimura, S.; Murata, K.; Akatsuka, W. Exceptionally High Glucose Current on A Hierarchically Structured Porous Carbon Electrode with "Eired" Flavin Adenine Dinucleotide-Dependent Glucose Dehydrogenase. *J. Am. Chem. Soc.* **2014**, *136*, 14432−14437.

(11) Murata, K.; Akatsuka, W.; Sadakane, T.; Matsunaga, A.; Tsujimura, S. Glucose Oxidation Catalyzed by FAD-Dependent Glucose Dehydrogenase within Os Complex-Tethered Redox Polymer Hydrogel. *Electrochim. Acta* **2014**, *136*, 537−541.

(12) Tsujimura, S.; Kojima, S.; Ikeda, T.; Kano, K. Potential-Step Coulometry of D-Glucose Using A Novel FAD-Dependent Glucose Dehydrogenase. *Anal. Bioanal. Chem.* **2006**, *386*, 645−651.

(13) Tsujimura, S.; Kojima, S.; Kano, K.; Ikeda, T.; Sato, M.; Sanada, H.; Omura, H. Novel FAD-Dependent Glucose Dehydrogenase for A Dioxygen-Insensitive Glucose Biosensor. *Biosci., Biotechnol., Biochem.* **2006**, *70*, 654−659.

(14) Hou, C.; Fan, S.; Lang, Q.; Liu, A. Biofuel Cell Based Self-Powered Sensing Platform for L-Cysteine Detection. *Anal. Chem.* **2015**, *87*, 3382−3387.

(15) Ravenna, Y.; Xia, L.; Gun, J.; Mikhaylov, A. A.; Medvedev, A. G.; Lev, O.; Alfonta, L. Biocomposite Based on Rreduced Graphene Oxide Film Modified with Phenothiazone and Flavin Adenine Dinucleotide-Dependent Glucose Dehydrogenase for Glucose Sensing and Biofuel Cell Applications. *Anal. Chem.* **2015**, *87*, 9567−9571.

(16) Yehezkeli, O.; Tel-Vered, R.; Raichlin, S.; Willner, I. Nano-Engineered Flavin-Dependent Glucose Dehydrogenase/Gold Nano-particle-Modified Electrodes for Glucose Sensing and Biofuel Cell Applications. *ACS Nano* **2011**, *5*, 2385−2391.

(17) Milton, R. D.; Giroud, F.; Thumser, A. E.; Minteer, S. D.; Slade, R. C. T. Hydrogen Peroxide Produced by Glucose Oxidase Affects The Performance of Laccase Cathodes in Glucose/ Oxygen Fuel Cells: FAD-Dependent Glucose Dehydrogenase as A Replacement. *Phys. Chem. Chem. Phys.* **2013**, *15*, 19371−19373.

(18) Milton, R. D.; Lim, K.; Hickey, D. P.; Minteer, S. D. Employing FAD-Dependent Glucose Dehydrogenase within A Glucose/ Oxygen Enzymatic Fuel Cell Operating in Human Serum. *Bioelectrochemistry* **2015**, *106*, 56−63.

(19) Sakuta, R.; Takeda, K.; Ishida, T.; Igarashi, K.; Samejima, M.; Nakamura, N.; Ohno, H. Multi-Enzyme Anode Composed of FAD-Dependent and NAD-Dependent Enzymes with A Single Ruthenium Polymer Mediator for Biofuel Cells. *Electrochem. Commun.* **2015**, *56*, 75−78.

(20) Monošík, R.; Stredanský, M.; Lušpai, K.; Magdolen, P.; Šturdík, E. Amperometric Glucose Biosensor Utilizing FAD-Dependent Glucose Dehydrogenase Immobilized on Nanocomposite Electrode. *Enzyme Microb. Technol.* **2012**, *50*, 227−232.

(21) Zafar, M. N.; Wang, X.; Sygmund, C.; Ludwig, R.; Leech, D.; Gorton, L. Electron-Transfer Studies with A New Flavin Adenine Dinucleotide Dependent Glucose Dehydrogenase and Osmium Polymers of Different Redox Potentials. *Anal. Chem.* **2012**, *84*, 334−341.

(22) Zafar, M. N.; Beden, N.; Leech, D.; Sygmund, C.; Ludwig, R.; Gorton, L. Characterization of Different FAD-Dependent Glucose Dehydrogenases for Possible Use in Glucose-Based Biosensors and Biofuel Cells. *Anal. Bioanal. Chem.* **2012**, *402*, 2069−2077.

(23) Yamazaki, T.; Okuda-Shimazaki, J.; Sakata, C.; Tsuya, T.; Sode, K. Construction and Characterization of Direct Electron Transfer-Type Continuous Glucose Monitoring System Employing Thermostable Glucose Dehydrogenase Complex. *Anal. Lett.* **2008**, *41*, 2363−2372.

(24) Yamashita, Y.; Ferri, S.; Huynh, M. L.; Shimizu, H.; Yamaoka, H.; Sode, K. Direct Electron Transfer Type Disposable Sensor Strip for Glucose Sensing Employing An Engineered FAD Glucose Dehydrogenase. *Enzyme Microb. Technol.* **2013**, *52*, 123−128.

(25) Daly, R.; Hearn, M. T. W. Expression of Heterologous Proteins in *Pichia pastoris*: A Useful Experimental Tool in Protein Engineering and Production. *J. Mol. Recognit.* **2005**, *18*, 119−138.

(26) Bretthauer, R. K.; Castellino, F. J. Glycosylation of *Pichia pastoris*-Derived Proteins. *Biotechnol. Appl. Biochem.* **1999**, *30*, 193−200.

(27) Yoshida, H.; Sakai, G.; Mori, K.; Kojima, K.; Kamitori, S.; Sode, K. Structural Analysis of Fungus-Derived FAD Glucose Dehydrogenase. *Sci. Rep.* **2015**, *5*, 13498.

(28) Muguruma, H.; Hoshino, T.; Matsui, Y. Enzyme Biosensor Based on Plasma-Polyemrized Film-Covered Carbon Nanotube Layer Grown Directly on A Flat Substrate. *ACS Appl. Mater. Interfaces* **2011**, *3*, 2445−2450.

(29) Muguruma, H.; Hoshino, T.; Nowaki, K. Electronically Type-Sorted Carbon Nanotube-Based Electrochemical Biosensors with Glucose Oxidase and Dehydrogenase. *ACS Appl. Mater. Interfaces* **2015**, *7*, 584−592.

(30) Arnold, K.; Bordoli, L.; Kopp, J.; Schwede, T. The SWISS-MODEL Workspace: A web-based environment for protein structure homology modelling. http://swissmodel.expasy.org/ (accessed October 21, 2016).